J|A|C|S
COMMUNICATIONS

Published on Web 02/22/2007

Thermally Driven Unidirectional Crystallization of Charged Colloidal Silica

Akiko Toyotama,[†] Junpei Yamanaka,*[,†] Masakatsu Yonese,[†] Tsutomu Sawada,[‡] and Fumio Uchida[§]

Faculty of Pharmaceutical Sciences, Nagoya City University, 3-1 Tanabe, Mizuho, Nagoya, Aichi 467-8603, Japan, National Institute for Materials Science, 1-1 Namiki, Tsukuba, Ibaraki 305-0044, Japan, and Fuji Chemical Co., Ltd., 1-35-1 Deyashiki-Nishi, Hirakata, Osaka 573-0003, Japan

Received November 17, 2006; E-mail: yamanaka@phar.nagoya-cu.ac.jp

Charged colloidal particles dispersed in water self-assemble into "crystal" structure, when the electrostatic interparticle interaction is sufficiently strong.[1] These colloidal crystals have received considerable attention as photonic crystals since their Bragg wavelengths usually lie in the visible light regime. Thus, ingenious crystallizations[2−5] have been developed to date. Here, we report a novel directed crystallization of dilute colloidal silica in coexistence with pyridine (Py), under a temperature gradient. This method enables the fabrication of well-oriented and large (1 mm × 10 mm × ∼30 mm) single-domain crystals in a short time (<10 min). Moreover, the crystals have sharp and deep transmission dips as well as good spatial uniformity in the Bragg wavelength λ_B (∼0.1%).

Thus far, sophisticated crystallizations, including shear annealing[3] and colloidal epitaxy,[4] have provided thin (thickness ≤0.1 mm) single-domain crystals with excellent uniformities and controlled orientations. Larger crystals (three-dimensional (3D), centimeter-sized) have been obtained from colloidal silica under a pH gradient[5] formed by the diffusion of Py or sodium carbonates; this is due to an increase of particle charge number with increase of pH, which results in charge-induced crystallization.[6] At present, however, the Bragg wavelengths of these 3D large crystals are more or less nonuniform (maximum of ∼10%). Thus, to date, it is still difficult to fabricate large colloidal single-domain crystals with good optical quality.

In ordinary crystalline materials, large single-crystals are produced by unidirectional solidification under a temperature gradient (e.g., Bridgman method). Although temperature T is a weak parameter for colloidal interactions,[1] it induces the crystallization of colloids indirectly. It has been reported that hard-sphere colloids exhibit thermally driven crystallization due to a gradient in the particle volume fraction, ϕ, which is generated by a gradient of T.[7]

For charged colloids, the gradients in electrostatic interaction magnitude, induced by T, should result in directed crystallization. An earlier study[8] showed that a homogeneous silica colloid containing Py crystallizes with increasing T and not solely by increasing [Py]; this was attributed to an enhanced dissociation of Py ($Py + H_2O \leftrightarrow PyH^+ + OH^-$, where PyH^+ denotes pyridinium cation) at high T and/or a reduction in the permittivity of water with increasing T. The crystallization was thermoreversible, and the crystallization temperature T_C, which was tunable near the room temperature T_R, was higher at lower [Py]. On the basis of this, here we examine the directed crystallization of the Py/silica system under a temperature gradient.

Aqueous colloidal silica (particle diameter = 110 nm; $\phi = 0.035$) was purified as described elsewhere.[5b] T_C was controlled by changing [Py]; at [Py] = 27.5 and 35 μM, T_C = 35 and 19 °C, respectively. Figure 1a illustrates the experimental setup. A colloid sample was introduced into a quartz cell (inner dimensions = 1 mm × 10 mm × 44 mm; wall thickness = 1 mm). The open end of the cell was sealed with plastic film, and the cell was placed horizontally to minimize the disturbance caused by convection on the crystal growth. Then, the other end of the cell was contacted with a copper heater block maintained at $T = T_0$. All the experiments were performed in a room thermostated at $T_R \approx$ 23 °C.

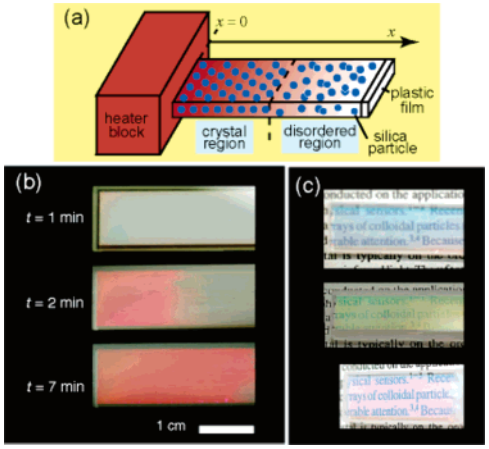

Figure 1. (a) Experimental setup; images of (b) crystallization process and (c) the single-domain crystal taken from different angles.

Figure 1b shows a typical crystallization process starting at time $t = 0$. We used a sample having T_C = 19 °C (<T_R) that had been cooled to 5 °C beforehand so that it took a disordered state; T_0 was 40 °C. The disordered region had an opaque appearance, while the crystal region exhibited a uniform diffraction color. Within 10 min the crystal length was a few centimeters. The cell was then separated from the heater block and equilibrated at T_R. Since $T_C < T_R$, the crystal structure was maintained, which facilitated further examinations. Figure 1c shows images of the crystal taken from three different angles. The diffraction color clearly exhibited an angular dependence, implying that the crystal was well oriented. Furthermore, the crystal had good transparency.

The optical property of the crystal was examined in greater detail by applying fiber-optic transmission spectrometry at various locations, x (Figure 1a); the measurements were performed in circular areas with diameters of ∼1 mm in a direction normal to the horizontal cell surface. Figure 2a depicts the spectra measured at x = 0−30 mm at 5-mm intervals (for the correspondence between the color of the spectrum curves and x values, cf. Figure 2b). The spectrum before the crystallization is shown in Figure 2a by the dashed curve for comparison. Enlarged spectra around the dips are shown in Figure 2a (inset). The crystal had sharp and deep dips at $\lambda_B \approx$ 616 nm, despite having a thickness of 1 mm; the half-dip

[†] Nagoya City University.
[‡] National Institute for Materials Science.
[§] Fuji Chemical Co., Ltd.

10.1021/ja0682327 CCC: $37.00

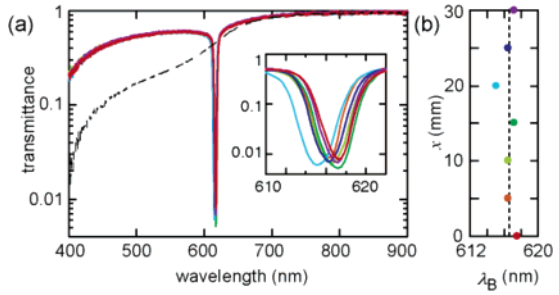

Figure 2. (a) Transmission spectra of the crystal at various locations (x = 0−30 mm; see text). Inset shows an enlarged view around the dips. (b) $\lambda_B - x$ plot.

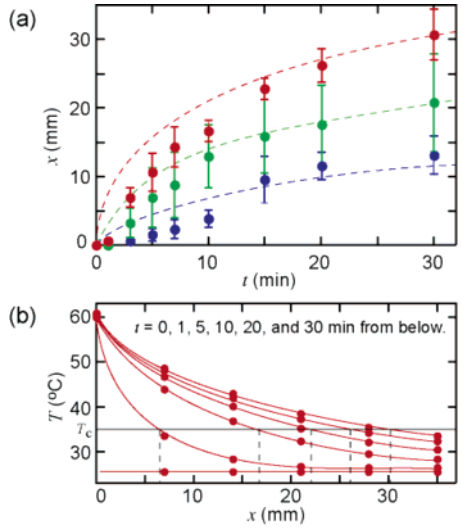

Figure 3. (a) Observed (symbols) and theoretical (dashed curves) crystal growths for T_0 = 40, 50, and 60 °C (shown in blue, green, and red, respectively). (b) Time evolution of $T(x)$ for T_0 = 60 °C. Locations of crystallization fronts at various t are represented by dashed vertical lines.

width was 5.8 nm on average, and the minimum transmittance reached nearly 0.005. These are comparable to the best results reported for thin crystals.[3] Furthermore, the crystal showed good optical uniformity over the entire region. Figure 2b represents the $\lambda_B - x$ plot; the dashed vertical line represents the averaged λ_B value. The variation of λ_B with x was 0.8 nm (0.1% of λ_B) in standard deviation. Laser diffraction experiments suggested that the present crystals had single-domain structures with normal or twin body-centered-cubic lattice symmetries, whose (110) planes were oriented parallel to the horizontal cell wall; details of the diffraction experiments are provided in Section A of the Supporting Information.

Charged colloids, as do hard-sphere colloids, may exhibit thermally driven crystallization due to a gradient in ϕ.[7] However, this mechanism is inapplicable here since λ_B (and thus, ϕ) was practically uniform. The crystallization mechanism was examined by comparing the crystal growth curves with the time evolution of temperature distribution $T(x)$. Here, we used a sample with T_C = 35 °C ($> T_R$) and chose T_0 = 40, 50, and 60 °C, whereby the growth rates clearly exhibited a dependence on T_0. Figure 3a shows the growth curves for the three T_0's; the bars represent the standard deviations of three runs. The growth rate increased with T_0, as expected from the larger heat-conduction rate. $T(x)$ was measured using an array of thermocouples attached to the outer surface of the cell at 7-mm intervals. Figure 3b represents the observed $T(x)$ at various t for T_0 = 60 °C; profiles at other T_0's are presented in Section B of the Supporting Information.

By assuming instantaneous crystallization at $T(x) = T_C$, we calculated the crystal length at various t (Figure 3b); this is represented by dashed curves in Figure 3a. They show close agreement with the experiments for all T_0, thereby suggesting that the present growth is attributed to a combination of heat conduction and thermally induced crystallization. We note that the thermal conductivity of the cell wall (quartz, 1.38 W/(m °C)) is larger than that of water (0.61 W/(m °C)), resulting in a lower T for the sample than that measured on the cell surface. The somewhat slower observed growths at $t \leq 10$ min might be due to this effect and/or the induction period for the nucleation of the crystal. The higher T on the cell surface might lead to formation of an oriented thin crystal layer, which acts as a crystallization template. It is likely that a combination of horizontal heat conduction in the colloid (the driving force of crystallization) and the wall effect (regulation of orientation) resulted in the well-oriented and large single-domain crystals.

Heat conduction is a diffusion of thermal energy, which is mathematically equivalent to, but can be much faster than, mass diffusion. Thus, the growth rate of the present crystallization could be much larger than that due to Py diffusion at constant T (less than a few mm/h).[5a] In the latter, the migration of particles during the growth period due to gravity and gradient of chemical potential may cause the nonuniformity in ϕ. The good uniformity attained in the present crystallization appeared to rely on its much faster growth rate. We expect the present method to be useful in fabricating photonic materials.

Acknowledgment. We sincerely thank Dr. Tsuyoshi Kano for his encouragements. This work was supported by the Grant-in-Aid for Research in Nagoya City University (to J.Y.).

Supporting Information Available: Additional details of the laser diffraction experiments and $T(x)$ at various t for T_0 = 40 and 50 °C. This material is available free of charge via the Internet at http://pubs.acs.org.

References

(1) (a) Russel, W. B.; Saville, D. A.; Schowalter, W. R. *Colloidal Dispersion*; Cambridge University Press; New York, 1989. (b) Sood, A. K. *Solid State Physics*; Ehrenreich, H., Turnbull, D., Eds.; Academic Press; New York, 1991. (c) Ise N.; Sogami, I. *Structure Formation in Solution*; Springer; Berlin, 2005.
(2) (a) van Blaaderen, A. *MRS Bull.* **2004**, 85−90. (b) Sullivan, M.; Zhao, K.; Harrison, C.; Austin, R. H.; Megens, M.; Hollingsworth, A.; Russel, W. B.; Cheng, Z.; Mason, T.; Chaikin, P. M. *J. Phys.: Condens. Matter* **2003**, *15*, S11−S18. (c) Schöpe, H. J. *J. Phys.: Condens. Matter* **2003**, *15*, L533−L540.
(3) (a) Clark, N. A.; Hurd, A. J.; Ackerson, B. J. *Nature* **1979**, *281*, 57−60. (b) Stipp, A.; Biehl, R.; Preis, T.; Liu, J.; Fontecha, A. B.; Schöpe, H. J.; Palberg, T. *J. Phys.: Condens. Matter* **2004**, *16*, S3885−S3902. (c) Kanai, T.; Sawada, T.; Toyotama, A.; Kitamura, K. *Adv. Funct. Mater.* **2005**, *15*, 25−29. (d) Toyotama, A.; Kanai, T.; Sawada, T.; Yamanaka, J.; Ito, K.; Kitamura, K. *Langmuir* **2005**, *21*, 10268−10270.
(4) (a) van Blaaderen, A.; Wiltzius, P. *Nature* **1997**, *385*, 321−324. (b) Hoogenboom, J. P.; Yethiraj, A.; van Langen-Suurling, A. K.; Romijn, J.; van Blaaderen, A. *Phys. Rev. Lett.* **2002**, *89*, 256104-1−256104-4.
(5) (a) Yamanaka, J.; Murai, M.; Iwayama, Y.; Yonese, M.; Ito, K.; Sawada, T. *J. Am. Chem. Soc.* **2004**, *126*, 7156−7157. (b) Wakabayashi, N.; Yamanaka, J.; Murai, M.; Ito, K.; Sawada, T.; Yonese, M. *Langmuir* **2006**, *22*, 7936−7941.
(6) (a) Yamanaka, J.; Koga, T.; Ise, N.; Hashimoto, T. *Phys. Rev. E* **1996**, *53*, R4314−4317. (b) Yamanaka, J.; Yoshida, H.; Koga, T.; Ise, N.; Hashimoto, T. *Phys. Rev. Lett.* **1998**, *80*, 5806−5809.
(7) Chen, Z.; Russel, W. B.; Chaikin, P. M. *Nature* **1999**, *401*, 893−895.
(8) Yamanaka, J.; Koga, T.; Yoshida, H.; Ise, N.; Hashimoto, T. *Slow Dynamics in Complex Systems*; Tokuyama, M., Oppenheim, I., Eds.; Woodbury: New York; 1998; p 144.

JA0682327